中南大学物理与电子学院
肖思 副教授
电话：18673123070

Dynamic self-diffraction in MoS_2 nanoflake solutions

Si Xiao,[1,2] Bosai Lv,[1] Liang Wu,[1] Menglong Zhu,[1] Jun He,[1] and Shaohua Tao[1,*]

[1]*Institute of Super-Microstructure and Ultrafast Process in Advanced Materials, School of Physics and Electronics, Hunan Key Laboratory for Super-Microstructure and Ultrafast Process, Central South University, Changsha 410083, China*

[2]*sixiao@csu.edu.cn*

[*]*eshtao@csu.edu.cn*

Abstract: We observe dynamic self-diffraction in MoS_2 supernatant solutions with laser for the first time, and conduct dynamic data simulation and analysis. Observation results indicate that self-diffraction can be divided in three stages: in the first stage, laser changes from Gauss beam to symmetric diffraction rings because of the force from laser. In the second stage, diffraction rings become asymmetric vertically because of gravity. In the third stage, diffraction rings become asymmetric horizontally, as a result of fine structure of laser. We obtain the dynamic distribution of MoS_2 nanoflake in solution under the effect of laser by dynamic diffraction image simulation.

OCIS codes: (350.4855) Optical tweezers or optical manipulation; (050.1940) Diffraction; (160.4236) Nanomaterials.

References and links

1. K. S. Novoselov, D. Jiang, F. Schedin, T. J. Booth, V. V. Khotkevich, S. V. Morozov, and A. K. Geim, "Two-dimensional atomic crystals," Proc. Natl. Acad. Sci. U.S.A. **102**(30), 10451–10453 (2005).
2. B. Radisavljevic, M. B. Whitwick, and A. Kis, "Small-signal amplifier based on single-layer MoS2," Appl. Phys. Lett. **101**(4), 043103 (2012).
3. D. Sarkar, W. Liu, X. Xie, A. C. Anselmo, S. Mitragotri, and K. Banerjee, "MoS2 field-effect transistor for next-generation label-free biosensors," ACS Nano **8**(4), 3992–4003 (2014).
4. Z. Yin, H. Li, H. Li, L. Jiang, Y. Shi, Y. Sun, G. Lu, Q. Zhang, X. Chen, and H. Zhang, "Single-layer MoS2 phototransistors," ACS Nano **6**(1), 74–80 (2012).
5. B. Radisavljevic, A. Radenovic, J. Brivio, V. Giacometti, and A. Kis, "Single-layer MoS2 transistors," Nat. Nanotechnol. **6**(3), 147–150 (2011).
6. B. Radisavljevic, M. B. Whitwick, and A. Kis, "Integrated circuits and logic operations based on single-layer MoS2," ACS Nano **5**(12), 9934–9938 (2011).
7. B. Radisavljevic, M. B. Whitwick, and A. Kis, "Correction to integrated circuits and logic operations based on single-layer MoS2," ACS Nano **7**(4), 3729 (2013).
8. K. Liu, J. Feng, A. Kis, and A. Radenovic, "Atomically thin Molybdenum Disulfide nanopores with high sensitivity for DNA translocation," ACS Nano **8**(3), 2504–2511 (2014).
9. G. Eda, H. Yamaguchi, D. Voiry, T. Fujita, M. Chen, and M. Chhowalla, "Photoluminescence from chemically exfoliated MoS2," Nano Lett. **11**(12), 5111–5116 (2011).
10. K. F. Mak, C. G. Lee, J. Hone, J. Shan, and T. F. Heinz, "Atomically thin MoS2: a new direct-gap semiconductor," Phys. Rev. Lett. **105**(13), 136805 (2010).
11. R. S. Sundaram, M. Engel, A. Lombardo, R. Krupke, A. C. Ferrari, P. Avouris, and M. Steiner, "Electroluminescence in single layer MoS2," Nano Lett. **13**(4), 1416–1421 (2013).
12. A. O'Neill, U. Khan, and J. N. Coleman, "Preparation of high concentration dispersions of exfoliated MoS2 with increased flake size," Chem. Mater. **24**(12), 2414–2421 (2012).
13. K. P. Wang, J. Wang, J. T. Fan, M. Lotya, A. O'Neill, D. Fox, Y. Y. Feng, X. Y. Zhang, B. X. Jiang, Q. Z. Zhao, H. Z. Zhang, J. N. Coleman, L. Zhang, and W. J. Blau, "Ultrafast saturable absorption of two-dimensional MoS2 nanosheets," ACS Nano **7**(10), 9260–9267 (2013).
14. W. Lee and C. S. Chiu, "Observation of self-diffraction by gratings in nematic liquid crystals doped with carbon nanotubes," Opt. Lett. **26**(8), 521–523 (2001).
15. Y.-J. Wang and G. O. Carlisle, "Optical properties of disperse-red-1-doped nematic liquid crystal," J. Mater. Sci. El. **13**, 173–178 (2002).

#226987 - $15.00 USD Received 18 Nov 2014; revised 12 Feb 2015; accepted 18 Feb 2015; published 25 Feb 2015

16. I.-C. Khoo, K. Chen, and Y. Z. Williams, "Orientational Photorefractive Effect in Undoped and CdSe Nanorods-Doped Nematic Liquid Crystal—Bulk and Interface Contributions," IEEE J. Sel. Top. Quantum Electron. **12**(3), 443–450 (2006).
17. M.-R. Lee, J.-R. Wang, C.-R. Lee, and A. Y.-G. Fuh, "Optically switchable biphotonic photorefractive effect in dye-doped liquid crystal films," Appl. Phys. Lett. **85**(24), 5822–5824 (2004).
18. Y.-P. Huang, T.-Y. Tsai, W. Lee, W.-K. Chin, Y.-M. Chang, and H.-Y. Chen, "Photorefractive effect in nematic-clay nanocomposites," Opt. Express **13**(6), 2058–2063 (2005).
19. H. C. Zhang, S. Shiino, A. Kanazawa, O. Tsutsumi, T. Shiono, and T. Ikeda, "Photoinduced reorientation and thermal effects in an oligothiophene-doped liquid crystal system," J. Appl. Phys. **91**(9), 5558–5563 (2002).
20. I. C. Khoo, H. Li, and Y. Liang, "Observation of orientational photorefractive effects in nematic liquid crystals," Opt. Lett. **19**(21), 1723–1725 (1994).
21. I. C. Khoo and T.-H. Lin, "Nonlinear optical grating diffraction in dye-doped blue-phase liquid crystals," Opt. Lett. **37**(15), 3225–3227 (2012).
22. W. Ji, W. Chen, S. Lim, J. Lin, and Z. Guo, "Gravitation-dependent, thermally-induced self-diffraction in carbon nanotube solutions," Opt. Express **14**(20), 8958–8966 (2006).
23. O. M. Maragó, F. Bonaccorso, R. Saija, G. Privitera, P. G. Gucciardi, M. A. Iatì, G. Calogero, P. H. Jones, F. Borghese, P. Denti, V. Nicolosi, and A. C. Ferrari, "Brownian motion of graphene," ACS Nano **4**(12), 7515–7523 (2010).
24. G. Wang, S. Zhang, F. A. Umran, X. Cheng, N. Dong, D. Coghlan, Y. Cheng, L. Zhang, W. J. Blau, and J. Wang, "Tunable effective nonlinear refractive index of graphene dispersions during the distortion of spatial self-phase modulation," Appl. Phys. Lett. **104**(14), 141909 (2014).
25. R. Wu, Y. Zhang, S. Yan, F. Bian, W. Wang, X. Bai, X. Lu, J. Zhao, and E. Wang, "Purely Coherent Nonlinear Optical Response in Solution Dispersions of Graphene Sheets," Nano Lett. **11**(12), 5159–5164 (2011).
26. A. B. Villafranca and K. Saravanamuttu, "Diffraction rings due to spatial self-phase modulation in a photopolymerizable medium," J. Opt. A, Pure Appl. Opt. **11**(12), 125202 (2009).
27. R. Karimzadeh, "Spatial self-phase modulation of a laser beam propagating through liquids with self-induced natural convection flow," J. Opt. **14**(9), 095701 (2012).

1. Introduction

A single layer of molybdenum disulfide (MoS_2) consists of two planes of hexagonally arranged S atoms and a hexagonal plane of Mo atoms. Week van der Waals forces held individual MoS_2 layers together. With its graphene-like layer structure, MoS_2 has gradually become one of the most-studied novel nano film materials [1]. And a wide range of applications has be studied, such as small signal amplifier [2], transistor [3–5], integrated circuit [6, 7], biomedicine [8], etc., with mature fabrication and manufacturing technique. Up to now, a variety range of prominent optical properties has been reported, such as strong photoluminescence [9, 10], photosensitiveness better than graphene [11], etc. Dispersion technique is the easiest method to fabricate high concentration exfoliated MoS_2 solution, and it has been used in industrial production.

In 2012, O'Neill A. *et al* gave dispersions of relatively thin MoS_2 have no observable defects in high concentration solution in the solvent N-methyl-pyrrolidone [12]. And in October, 2013, Wang K P et al published their research in nonlinear optical property of MoS_2 with N-methyl-pyrrolidone, N-Vinyl-2-pyrrolidone and N-Cyclohexyl-2-pyrrolidone as solvent on *ACS nano* [13]. However, the effect of laser-cause self-diffraction would not be ignored in the research of nonlinear optical property in MoS_2 supernatant solutions.

In researches of liquid crystals, electric, magnetic, and optical field are used to modulate the orientation of liquid crystal molecules to study self-diffraction effect [14–20]. In 2012, Khoo I. C. *et al* observed strong nonlinear self-diffraction in methyl-red-dye doped liquid crystal sample with low-power cw lasers [21]. In such process, dye molecules director axis reorientation, disorder, and lattice distortion are excited by laser. However, the concentration change of sample due to gravity has not been taken in to consideration yet.

In 2006, Wei Ji *et al* published their research in a kind of Gravitation-dependent, thermally-induced self-diffraction in carbon nanotube solutions [22] on *Optics Express*. Prof. Ji focused continuous-wave laser beam onto a CNT solution and obtained observable self-diffraction spot after the laser beam propagates through the solution. They got average molecular weights of CNTs with doing simulations of diffraction pattern vertically. However, he only does static observation with negligible later research. The focused laser might account

#226987 - $15.00 USD Received 18 Nov 2014; revised 12 Feb 2015; accepted 18 Feb 2015; published 25 Feb 2015

for such limitation of their work. Because laser is focused on CNT solution, the area of the solution laser can act on is relatively limited. Under such circumstance, the time of self-diffraction forming process might be too short to observe.

In this study, we investigate dynamic self-diffraction in MoS_2 solutions with pules laser for the first time. In the experimental system, we employed high frequency (80MHz) pules laser to enhance laser power and use no lens creatively. And just because the incident laser beam is not focused, the area that laser can actually act on is greatly expanded. As a result, the forming time of self-diffraction is extended to 10-second scale, which makes the three stages in the forming process observable and analysis of inner main mechanism of each stage possible. Through analysis of finishing times of every stage and final state observation, the internal relation between the speed of dynamic self-diffraction and laser power, solution viscosity and concentration of MoS_2 nanoflake solution can be qualitatively demonstrated. In the attempt of dynamic diffraction pattern simulation, we obtain the rough dynamic distribution of MoS_2 nanoflake in solution under laser effect. In this process, Computer-Generated Hologram (CGH) and Gerchberg-Saxton (GS) are first used to study the distribution of MoS_2 in solution. The paper provides experimental method and fundamental research for later study of observation and research in the interaction between laser and suspending nanoparticle in solution.

2. Experiment: methods and results

MoS_2 supernatant solutions were fabricated with dispersion method used in Reference paper [12] with N,N-Dimethylformamide (DMF) and N-methyl-pyrrolidone (NMP) as solvent. The range of MoS_2 solution concentration used in the experiment is 0.1mg/ml to 1mg/ml. Double beam scanning electron microscope FEI Helios Nanolab 600i was employed to measure the size of MoS_2 nanoflake. AFM scanning was conducted in ambient with Agilent 5500AFM/SPM. Contact mode and silicon probes with a 10nm radius of curvature (NCLV-A bought from Bruker) were used. Size of quartz cells is 10x10mm.

In this self-diffraction experiment, laser resource was Tsunami 3941-30-X1S ultrafast oscillators system from Spectra-Physics, Newport Corporation. Output Characteristics of the system are: Tuning Range 780-820nm, Pulse Width <30 fs, Repetition Rate 80 MHz. Incident laser was not focused. The detector was Visible Laser Beam Profiler(LBP-2-USB) from Newport Corporation. Its wavelength range is 350-1100nm.

Schematic diagram Figs. 1(a) and 1(b) shows two kinds of set-ups used in the experiment with quartz cell placed horizontally and vertically, respectively. In Fig. 1(a), the sample, MoS_2 with DMF as solvent, was placed at an angel of 16.7° with the horizontal. Incident pules laser traveled into MoS_2 solution vertically. While output laser was received by detector, the self-diffraction pattern with sample placed obliquely. In Fig. 1(b), the sample carrying the same kind of solution was placed vertically, and incident laser was perpendicular to one of quartz cell walls. The self-diffraction pattern was received when output laser get in the detector.

Figures 1(c) and 1(d) show diffraction patterns when laser power was 220mW, wavelength was 820nm with sample placed obliquely and vertically, respectively. It's easy to see that diffraction pattern shows in Fig. 1(c) consists of a series of concentric rings with no rings at central area of diffraction pattern. Under condition same as that in Fig. 1(c), output laser spots were typical Gaussian spots with on sample in the optical path, no solution in the quartz cell and pure solvent as sample. These evidences demonstrate that self-diffraction effect causes by some unique proprieties of MoS_2 and has nothing to do with set-ups, quartz cells and solvents. It's easy to notice that diffraction pattern is distorted in Fig. 1(d) that have no rings at top half and brighter rings at bottom half. Diffraction pattern in Fig. 1(d) is stretched vertical which shows the gravity effect in the formation of self-diffraction. Researchers also studied effect of laser power and solution concentration on self-diffraction effect. These experiments were conducted with the method used in reference paper [22]. In these experiments, researchers

#226987 - $15.00 USD Received 18 Nov 2014; revised 12 Feb 2015; accepted 18 Feb 2015; published 25 Feb 2015

found that considerable laser power is needed for observable self-diffraction and more significant self-diffraction effect with larger number of brighter rings can be observed with higher MoS_2 solution concentration. Videos of dynamic self-diffraction processes from appearance to stable were recorded with detector film-recording function on and shutter speed controlled to be consistent to time of incident laser. Figure 1(e) is SEM image of MoS_2 nanoflake in MoS_2 supernatant solutions which shows the scale of MoS_2 nanoflake is relatively even and is range from 5μm to 10μm. The AFM image in Fig. 1(f) shows the thickness of MoS_2 nanoflake is range from 100nm to 200nm. Researchers conducted several experiments of a variety of dielectric nanoparticle, including MgO nanoparticle, Al_2O_3 nanoparticle, copper nanoparticle (diameter: 3μm), $Al(OH)_3$ nanoparticle, polystyrene microsphere, and TIO_2 powder in water, and Ag nanowire in ethanol, with relatively smaller SVR in solution to obtain self-diffraction, but fail. These experiments indicate that large surface-to-volume ratio (SVR) of Quasi-two-dimensional material, MoS_2 nanoflake (SVR = 4.81 x 106/m), is the key factor to obtain self-diffraction. Nanomaterial with large surface can sustain more force from laser. Furthermore, relatively light weight helps itself to be drove by laser and forms diffraction screen.

2.1 Dynamic self-diffraction process with sample placed obliquely and analysis

Images in Fig. 2 are screenshots of the video of dynamic self-diffraction process MoS_2 in DMF with sample placed at an angel of 16.7° with the horizontal. Pules laser went through the solution from up to down vertically, laser power was 180mW. The specific time from beginning of video recording to appearance of every image is marked at bottom of each image. Observation results indicate that self-diffraction can be divided in two stages: in the first stage (1.64s~2.64s), laser changes from Gauss beam to symmetric diffraction rings. The radius of diffraction pattern expands, more rings emerge and the shape changes from perfect circles to ellipses which are symmetric both vertically and horizontally. In the second stage, diffraction rings become asymmetric vertically, while they are symmetric horizontally. Sizes and number of diffraction rings tend to be stable. The diffraction rings gradually appear to be slightly compressed in the top half of the rings and stretched in the bottom half.

This effect can be explained by optical tweezers theory. The force causes by interaction of laser and dielectric particle at nanometer or micrometer scale can be pico-Newton scale and can be used to move dielectric particle. In 2010, O. M. Marago *et al* reported to trap graphene flake with optical tweezers [23]. Although incident laser beam used in experiment mentioned above is not focused, transient laser power per unit area of femtosecond pules laser would reach 1.27×10^{14} mW/m^2, at the same scale as that of laser used in experiments by O. M. Marago *et al*.

As the fact that no diffraction rings appear at the central area of diffraction patterns, the classical diffraction theory tell us central area of diffraction pattern would appear to be dark if the diffraction screen is opaque which agrees with this self-diffraction effect. Hence, the conjecture would be: MoS_2 nanoflake in solution are attracted to and collect at the center of laser beam, if laser power reaches some specific level. Then the opaque diffraction screen forms.

Specific explanation is as follows. The first stage of self-diffraction is dominated by force of laser. And it also affected by gravity. The moment laser travels into the solution, MoS_2 nanoflakes are still not ready to react on it to move towards the center of laser beam, so it can be assumed that laser beam propagates straight through the solution and typical Gaussian spot is received, in Fig. 2(a). Then MoS_2 nanoflakes around the laser path begin to move at the direction of the laser beam center. In this way, as time goes by, opaque diffraction screen gradually forms at the laser beam center and diffraction pattern is received, in Fig. 2(b). As more nanoflakes accumulate at the laser beam center, area of diffraction screen expands and radius and number of diffraction rings increases, as images show in Figs. 2(c)-2(e). Then due to the limitation of laser power, when the controlling force reaches its limitation, diffraction

#226987 - $15.00 USD Received 18 Nov 2014; revised 12 Feb 2015; accepted 18 Feb 2015; published 25 Feb 2015

screen comes to be stable, radius and number of diffraction ring become stable as a result, in Fig. 2 (f).

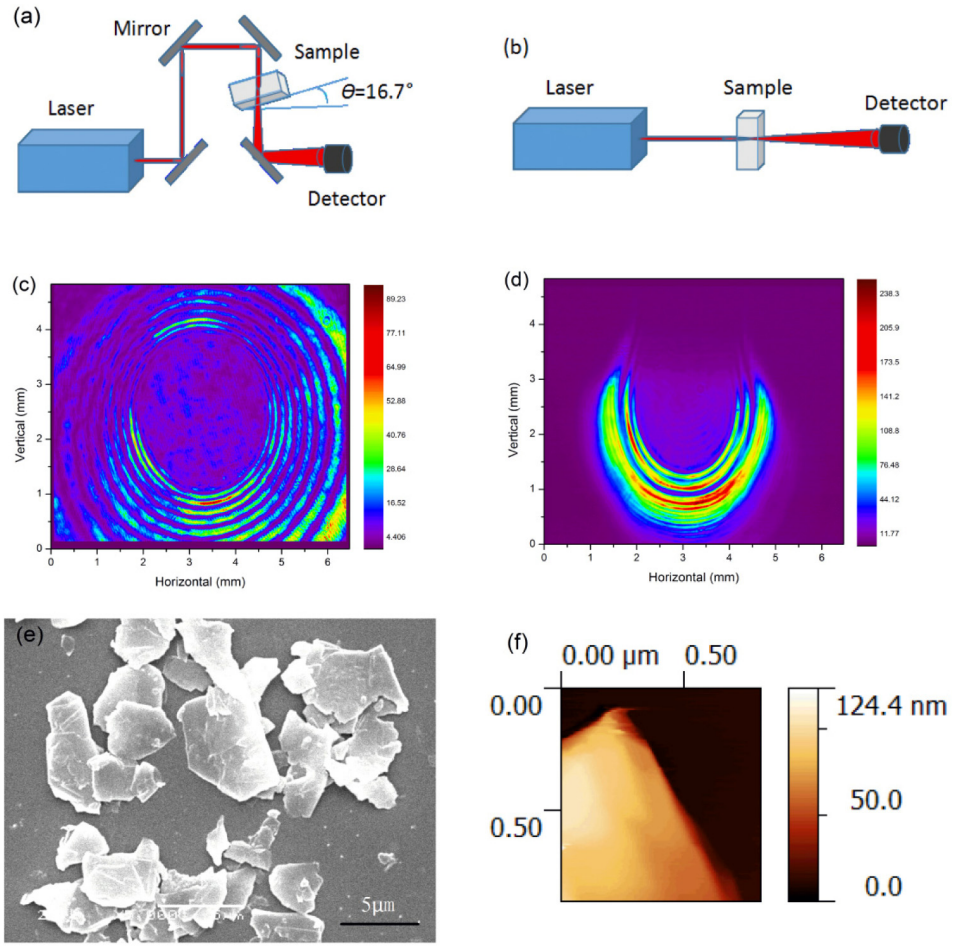

Fig. 1. Self-diffraction in Molybdenum disulðde solutions. SEM image and AFM topography image of molybdenum disulfide. (a) Schematic diagram shows the set-up with the sample placed at an angel of 16.7° with the horizontal; (b) Schematic diagram shows the set-up with the sample placed vertically; (c) and (d) are the typical diffraction patterns observed at 820 nm with the set-ups shown in (a) and (b), and the input laser powers used are 220mW, respectively. (e) and (f) are SEM and AFM images of MoS_2 used in the experiment, respectively.

From lasers get into solution to the first stage finishes, both the force of laser (dominating) and viscous force of solution contribute to the primary mechanism. Factors determine the finish time of the first stage of self-diffraction are the force of laser beam (determined by power of laser), viscosity coefficient of different kind of solvent and concentration of MoS_2 solutions. Higher laser power means stronger controlling force, and less time is needed to reach stable condition; if MoS_2 nanoflakes are in solvent with higher viscosity coefficient, longer time are needed to reach stable because of bigger viscous force; if MoS_2 solution get higher concentration, time needed to reach stable would decreases due to controlling force of laser reaches its limitation easier. These conjectures are proved one by one in the following experiments as information shows in Table 1, Table 2 and Table 3. In Table 1, as times of the first stage with different laser powers, the first stage time with laser power of 180mW is 53% to that of laser power of 80mW. Table 2 and Table 3 record the first stage time when DMF and

#226987 - $15.00 USD Received 18 Nov 2014; revised 12 Feb 2015; accepted 18 Feb 2015; published 25 Feb 2015

NMP are used as solvent respectively, with concentration of 1mg/ml. When the same power of laser are used, the time of the first stage of self-diffraction with DMF as solvent (DMF viscosity coefficient is 0.802 mPa·s, 25°C) is 75% to that with NMP as solvent (NMP viscosity coefficient is 1.65 mPa·s, 25°C). Moreover, as data in Table 1, When the same power of laser and solvent (DMF) are used, the time of the first stage of this dynamic process with solution concentration of 1mg/ml is 50% to that with concentration of 0.25mg/ml.

After the first stage, it is the second stage that is determined by controlling force of laser and gravity. Due to laser controlling force reaches saturation, collected MoS_2 nanoflakes gradually tend to obey Boltzmann distribution vertically subject to the force of gravity. Because the inclination angle of sample is relatively small, the diffraction screen is slightly asymmetric vertically which causes the distorting of diffraction rings: slightly compressed in the top half of the rings (distances between rings decrease) and stretched in the bottom half (distances between rings increase), images show in Figs. 2(g)-(i). Compared to the changes of diffraction patterns show in Figs. 3(e)-(g) with sample placed vertically other factors unchanged, the distortion of diffraction rings (asymmetric vertically) with sample place obliquely is much less obvious, which can demonstrate the effect of gravity in the second stage.

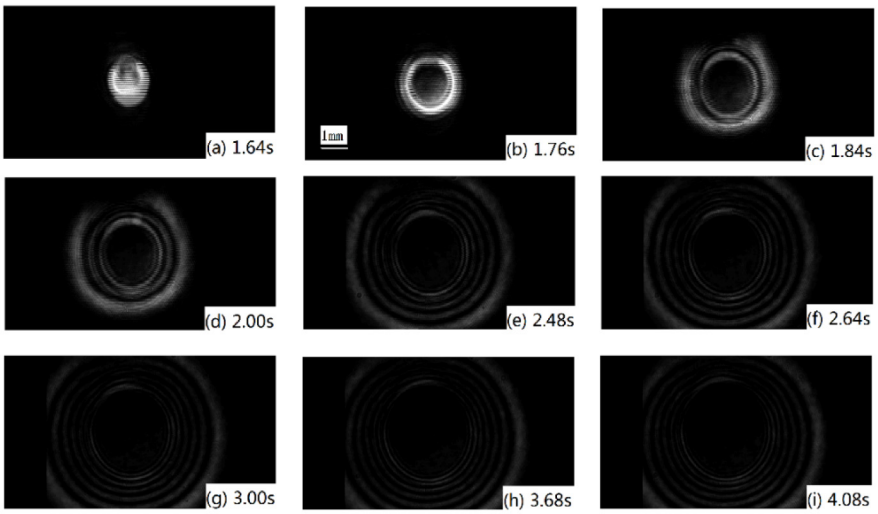

Fig. 2. Image (a) to image (i) show variations of diffraction patterns over time when the laser entered the solution with the sample placed at an angel of 16.7° with the horizontal. The incident laser power was 180mW. Under each image is the interval from the beginning of timing to the time it was recorded. As we can see, the process of dynamic self-diffraction includes two phases: the first phase, the radius of diffraction pattern expanded, more rings emerged and the shape changed from perfect circle to ellipse (1.64s ~2.64s); the second phase: the diffraction rings gradually appeared to be slightly compressed in the top half of the rings and stretched in the bottom half (2.64s ~4.80s).

Hence, conjecture of inner mechanism in solutions at the second stage is the combined effect of the force of laser and gravity. Factors determine the finish time of the second stage of self-diffraction are the force of laser beam (determined by power of laser) and viscosity coefficient of different kind of solvent. Higher laser power means stronger controlling force that would resist further movement of MoS_2 nanoflakes to follow the Boltzmann distribution, so more time is needed to reach stable state; if MoS_2 nanoflakes are in solvent with higher viscosity coefficient, longer time are needed to reach stable because of bigger viscous force; These conjectures are proved one by one in the following experiments as information shows in Table 1, Table 2 and Table 3. In Table 1, as times of the second stage with different laser

#226987 - $15.00 USD Received 18 Nov 2014; revised 12 Feb 2015; accepted 18 Feb 2015; published 25 Feb 2015

powers, the second stage time with laser power of 180mW is 173% to that of laser power of 80mW. Table 2 and Table 3 record the second stage time when DMF and NMP are used as solvent respectively, with concentration of 1mg/ml. When the same power of laser are used, the time of the second stage of self-diffraction with DMF as solvent is 94% to that with NMP as solvent.

If observe the images of that dynamic process more carefully, the third stage might be found: after the second stage, diffraction pattern might became to be asymmetric horizontally, as image showed in Fig. 2(i). This appearance would be discussed in the following part of analysis dynamic self-diffraction with sample placed vertically and conditions unchanged.

Table1,time and need time of every stage for dynamic self-diffraction with different laser power, 180mW and 80mW respectively, sample placed oblique. Solution concentration is 1mg/ml.

Kind of solvent,concentration of solution,Power of laser	DMF;1mg/ml; 180mW	DMF; 1mg/ml; 80mW
Appearance of laser spot (s)	1.610 ± 0.040	2.400 ± 0.040
Spot changes to ellipse (s)	2.600 ± 0.080	4.266 ± 0.080
Vertically asymmetric Horizontally symmetric(s)	4.800 ± 0.160	5.533 ± 0.200
Time needed for the first stage (s)	0.990 ± 0.120	1.866 ± 0.120
Time needed for the second stage (s)	2.200 ± 0.200	1.267 ± 0.240

2.2 Dynamic self-diffraction process with sample placed vertically and analysis

In this experiment, dynamic self-diffraction of MoS_2 solutions at different concentrations in DMF was studied with sample placed vertically and other condition unchanged. Images in Fig. 3 and Fig. 4 are screenshots of the video of dynamic self-diffraction process of MoS_2 solutions in DMF with sample placed vertically with pules laser going through the solution horizontally, laser power was 240mW. Solution concentrations were 1mg/ml and 0.25mg/ml, respectively. Videos recording started at the same time of laser beginning to interact with solution. Gaussian spot was not recorded in Fig. 3(a), because the image was taken as the process of removing the shutter away. Because sample was placed vertically, influence on distribution of MoS_2 nanoflakes of gravity turn to be more significant. The specific time from beginning of video recording to appearance of such image is marked at bottom of each image. Observation results indicate that self-diffraction can be divided in three stages: the first stage is approximately the same as that with sample placed obliquely, laser spot changed from Gaussian spot to concentric circle rings, and then became to be ellipse. This might because the vertical placement of sample, the effect of gravity becomes to be more significant. In the second stage, diffraction rings expanded and reached their maximum radius. Then diffraction rings shrunk slightly. At the same time top half of rings gradually faded away. Diffraction rings changed into half-moon shape. Rings became brighter and number of rings decreases simultaneously. This might also because the vertical placement of sample, the distribution of MoS_2 follows the Boltzmann distribution and the density of MoS_2 change to vertical direction become to be more obvious on cross section of laser beam. In other words, the effect of gravity becomes to be more significant. As a result asymmetry of diffraction patterns becomes more obvious. The first two stages can be explained by the mechanism above.

#226987 - $15.00 USD Received 18 Nov 2014; revised 12 Feb 2015; accepted 18 Feb 2015; published 25 Feb 2015

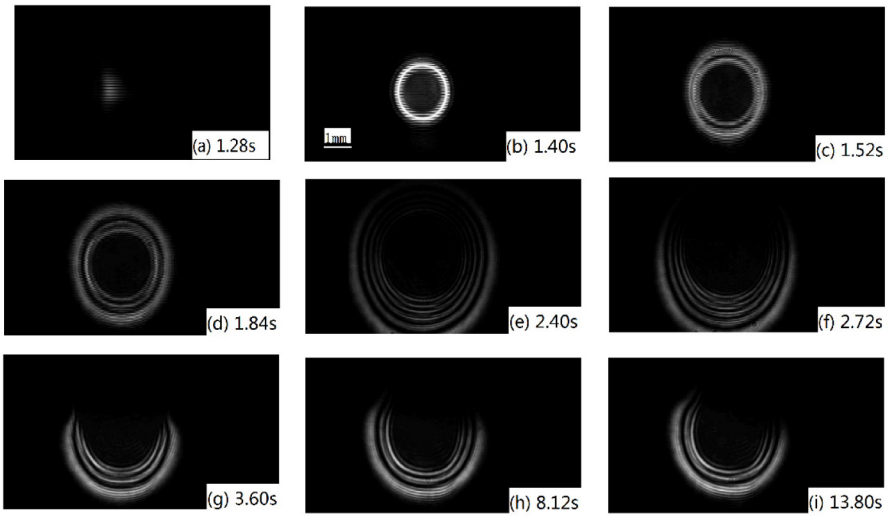

Fig. 3. Image (a) to image (i) show variations of diffraction patterns over time when the laser enter the 1mg/ml MoS_2 solution in DMF with the sample placed vertically. The incident laser power was 240mW. Under each image is the interval from the beginning of timing to the time it was recorded. As we can see, the process of dynamic self-diffraction includes three phases: the first phase, the radius of diffraction pattern expanded, more rings emerged and the shape changed from perfect circle to ellipse (1.28s~1.84s); the second phase: the top half of the diffraction pattern faded away, and the number of diffraction ring reduced (1.84s~3.60s); the third phase: diffraction rings gradually became asymmetric horizontally with no change in number of diffraction rings (3.60s~13.80s).

It's worth noting that the third stage comes up in the experiment. In the third stage, diffraction rings gradually became asymmetric horizontally with no change in number of diffraction rings. This asymmetry might because the distribution of laser power does not follow the Gaussian distribution. The fine structure of laser determines the controlling ability on every point of cross section of laser beam; and the slightly difference of MoS_2 distribution can be reflect on macroscopic diffraction pattern. Hence, according to this theory, macroscopic laser transmission diffraction pattern (at centimeter scale) observe by common CCD might be used to deduce the fine structure of incident laser (scale from millimeter to micrometer).

According to the comparison of dynamic self-diffraction with two kind of concentrations of solution, changing speed of self-diffraction with 1mg/ml MoS_2 solution is obviously higher than that of 0.25mg/ml. Specific times of every stage show in Table 2. The table recorded times of the appearance of laser spot, changing from spot to ellipse, rings becoming to be vertically asymmetric and rings becoming to be horizontally asymmetric with different kind of solution concentrations. Moreover, times that needed for every stage to finish are also calculated and added to the table.

According to the data in Table 2, time for the first stage with 1mg/ml solution to finish is only 50% to that with 0.25mg/ml solution. For the second stage, the former is 78.6% to the latter. The whole time for the first two stages of the former is 68.2% to the latter.

#226987 - $15.00 USD Received 18 Nov 2014; revised 12 Feb 2015; accepted 18 Feb 2015; published 25 Feb 2015

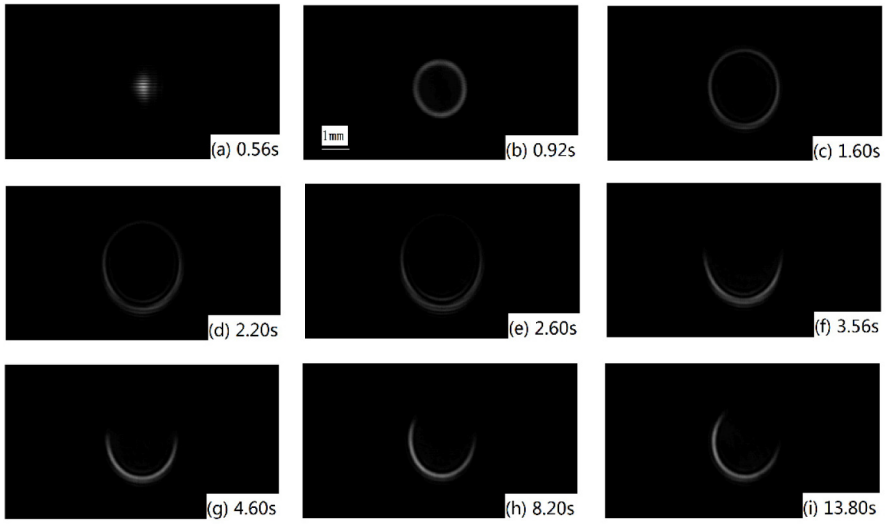

Fig. 4. Image (a) to image (i) show variations of diffraction patterns over time when the laser entered the 0.25mg/ml MoS_2 solution in DMF with the sample placed vertically. The incident laser power was 240mW. Under each image is the interval from the beginning of timing to the time it was recorded. As we can see, the process of dynamic self-diffraction includes three phases: the first phase, the radius of diffraction pattern expanded, more rings emerged and the shape changed from perfect circle to ellipse (0.56s~1.60s); the second phase: the top half of the diffraction pattern faded away, and the number of diffraction ring reduced (1.60s~4.60s); the third phase: diffraction rings gradually became asymmetric horizontally with no change in number of diffraction rings (4.60s~13.80s).

Table 2. ,time and need time of every stage for dynamic self-diffraction with different concentrations of solution in DMF, 1mg/ml and 0.25mg/ml respectively, sample placed vertically. Power of laser is 230mW.

Kind of solvent; concentration of solution	DMF;1mg/ml	DMF;0.25mg/ml
Appearance of laser spot (s)	1.266 ± 0.040	0.466 ± 0.040
Spot changes to ellipse (s)	2.066 ± 0.080	2.066 ± 0.080
Vertically asymmetric Horizontally symmetric(s)	4.266 ± 0.080	4.866 ± 0.080
Horizontally asymmetric (s)	13.866 ± 0.200	12.733 ± 0.240
Time for the first stage to finish(s)	0.800 ± 0.120	1.600 ± 0.120
Time for the second stage to finish (s)	3.000 ± 0.120	4.400 ± 0.120
Time for the three stage to finish(s)	12.600 ± 0.240	12.267 ± 0.240

Table 3. ,time and need time of every stage for dynamic self-diffraction with different concentrations of solution in NMP, 1mg/ml and 0.67mg/ml respectively, sample placed vertically. Laser power is 230mW

Kind of solvent; concentration of solution	NMP;1mg/ml	NMP;0.67mg/ml
Appearance of laser spot (s)	–0.180 ± 0.120	0.140 ± 0.040
Spot changes to ellipse (s)	0.866 ± 0.060	1.266 ± 0.120
Vertically asymmetric Horizontally symmetric(s)	3.200 ± 0.120	4.200 ± 0.160
Horizontally asymmetric (s)	11.866 ± 0.240	11.333 ± 0.200
Time for the first stage to finish(s)	1.066 ± 0.180	1.126 ± 0.160
Time for the second stage to finish (s)	3.400 ± 0.240	4.060 ± 0.200
Time for the three stage to finish(s)	12.066 ± 0.360	11.193 ± 0.240

#226987 - $15.00 USD Received 18 Nov 2014; revised 12 Feb 2015; accepted 18 Feb 2015; published 25 Feb 2015

2.3 The theoretical analysis of dynamic self-diffraction

The steady-state theory analysis of self-diffraction is reported by many papers [24, 25]. However, analysis of dynamic self-diffraction is rare. In 2009, Kalaichelvi Saravanamuttu et al discussed the non-reversible dynamic changes of symmetric self-diffraction ring in number and radius with solid photopolymerizable organosiloxane medium in the 45s with a cw laser [26]; 2012, R Karimzadeh theoretical simulation of self-diffraction rings with dye in ethanol as solution and a low power cw laser in the 1s changes over time. Its diffraction rings are upper and lower asymmetric and bilaterally symmetric. However, the consistent between simulation results and experiment results is not very satisfactory [27]. But so far, this is the first time to found that dynamic self-diffraction can be divided into three stages and to analyze the time of three stages. Up to now, several mechanisms are involved in the analysis of self-diffraction in the liquid, and no conclusive theory has been come up. This theoretical research focused on the rough formula of characteristic completion time of every stage and laser force, gravity and fluid resistance.

To simplify the discussion, only changes of diffraction fringes in vertical direction are discussed considering upper and lower asymmetric and bilaterally symmetric changes in the first and second stages. The MoS_2 density in this direction is set as $\rho(x=0,y,t)$. The Fokker–Planck equation of motion for the density has the form of:

$$\frac{\partial \rho}{\partial t} = -\nabla \bullet \vec{j}_f + D\nabla^2(\rho) \tag{1}$$

where $-\nabla \bullet \vec{j}_f$ is the drift term, $D\nabla^2(\rho)$ is the diffusion term, D is the diffusion constant,and $\vec{j}_f$ is the density current. Referring to the "mobility" definition $\mu = V/F$ (the ratio of the particle's terminal drift velocity to an applied force) and the Einstein relation $D = \mu k_B T$,the density current can be given as $\vec{j}_f = \rho\mu\vec{f} = \frac{D\rho}{K_B T}\vec{f}$,where k_B is Boltzmann's constant; T is the absolute temperature. $\vec{f}$ is the total external force, including the optical and gravitational force, hence, $\vec{f} = \nabla f_L(I) - \rho g\hat{y}$. $f_L(I) = \frac{ns}{c} I(x=0,y,t)$ is the force laser acting on MoS_2, n is the refraction index, c is the speed of light in vacuum, s is the light receiving area for MoS_2. $I(x=0,y,t)$ is the laser intensity irradiated on MoS_2. The center light intensity is higher following Gaussian distribution. Therefore, the laser gradient force is centripetal, which tends to push MoS_2 towards the laser spot center. g is the gravitational acceleration which characterizes gravity. The direction of gravity is always along the negative y-axis direction.

If MoS_2 is kept free from the action of external force or there is a balance of the external force $\vec{f} = 0$, Fokker–Planck Eq. (1) reduces to the conventional heat equation, whose fundamental solution is $\rho(r,t) = \frac{1}{\sqrt{4\pi Dt}} e^{-\frac{r^2}{4Dt}}$,which means when density distribution ρ reaches a particular state, Dt would be a constant. Therefore we have the characteristic time of diffusion $T_D \propto 1/D$. Based on Stokes-Einstein equation $D = \frac{k_B T}{6\pi\eta r}$ η is the dynamic viscosity; r is the radius of the spherical particle, we have $T_D \propto \eta$. Hence, the time needed to establish equilibrium is proportional to η . In other words, the solution with higher value of η , the longer time is needed to reach equilibrium. This conclusion is consistent with the time

#226987 - $15.00 USD Received 18 Nov 2014; revised 12 Feb 2015; accepted 18 Feb 2015; published 25 Feb 2015

regularity with 1mg / ml MoS_2 solution in DMF or NMP in the first and second stage shown in table2 and table3, under 230mW laser irradiation. But the effective value of η is dependent on concentration, and solvent property of suspension solution, which would enhance the complexity of this problem.

Considering the impact of light intensity: the first stage begins immediately when the laser is irradiated on the sample, MoS_2 follows Boltzmann distribution in solution, and the influence of gravity is negligible in solution. Affected by the laser light intensity distribution, the MoS_2 density distribution will approach Gaussian distribution from Boltzmann distribution. The initial deviation is created by the optical excitation and the following relaxation time is also determined by the optical intensity. Due to the exponential form of the decay function, the characterization time $T_D \propto 1/I$. This conclusion roughly agrees with the first stage completion time of diffraction 1.0s/1.9s in table1 in solution with DMF as solvent and laser powers are 180mW and 80mW, respectively. At the beginning of the second stage, the distribution of MoS_2 in solution tend to follow Gaussian distribution, and the force of laser tends to reach saturation. The density center moves downward under the force of gravity, and the laser gradient force is acting against this process. Therefore,in this stage, the characterization time $T_D \propto I$,This conclusion basically agrees with the second stage completion time of diffraction 2.2s/1.3s in table1 in solution with DMF as solvent and laser powers are 180mW and 80mW, respectively.

Concentration ρ in Eq. (1) would affect several aspects. Higher concentration can: reduce the value of η ; enhance the increase of density current effectively; let more particles in the irradiation area of laser and more particles would be trapped by laser; may enhance the refractive index n ;And all of impacts can help to reduce T_D efficiently, which agree with the experimental results.

In the third stage, both the force of laser and gravity have already reached their saturations. And at this time, the driving term, the laser gradient force $\vec{f} = \nabla f_L(I)$ due to the fine structure of laser is very week, so the time needed to reach steady state would exceeds 10 seconds. As a result, left-right asymmetry of self-diffraction pattern is produced.

2.4 The simulation of dynamic MoS_2 distribution in solution in the dynamic self-diffraction process

The intensity and phase of diffracted light of laser when it travel through the MoS_2 solution is determined by the distribution of MoS_2 nanoflake in solution which acts like a spatial light modulator (SLM). Hence, we can obtain the three-dimensional distribution of MoS_2 by deducing the phase change with the linear relationship between MoS_2 population density and the phase change. Therefore, a distribution detecting method is used in this study to recover the three-dimensional distribution of MoS_2 with specific diffraction patterns. At the beginning, a wavefront function involving the phase change of MoS_2 solution is retrieved from the intensity of the incident light and the diffraction light based on the GS algorithm. Next, with the help of a gradient field based phase estimation algorithm to overcome the phase wrapping problem, the phase change of the solution is obtain from the calculation of the retrieved wavefront function. And finally, by constructing a linear model between the MoS_2 distribution and the phase change, the three-dimension distribution of MoS_2 in solution is calculated from the obtained solution phase change.

With this method, dynamic MoS_2 nanoflakes distribution in solution in the second stage with sample placed vertically is retrieved from the dynamic diffraction patterns. And that could help with further understanding of the inner mechanism of the dynamic self-diffraction phenomenon. Figure 5(a) is the original distribution of MoS_2 in solution. Screenshots of dynamic self-diffraction video show in Figs. 4(b)-4(i) are used to retrieve the MoS_2 dynamic

#226987 - $15.00 USD Received 18 Nov 2014; revised 12 Feb 2015; accepted 18 Feb 2015; published 25 Feb 2015

distribution show in Figs. 5(b)-5(i), respectively. Moreover, the calculated dynamic distribution of MoS2 show in Fig. 5 is used to calculate the corresponding diffraction pattern. And surprisingly, diffraction patterns calculated based on previous distributions results have a great match of the diffraction patterns show in Fig. 4 which means the simulation is of high accuracy. This would be a further prove the diffraction mechanism introduced in this paper. It is easy to notice that MoS_2 assembling center moves at the direction of gravity over time in the second stage, as Figs. 5(c)-5(g) show. Figures 5(g)-5(i) are the simulation images of the third stage, the assembling center moves horizontally because of the fine structure of laser beam. According to the discussion above, both the force of laser and gravity contribute to the mechanism in the second stage. Due to laser controlling force reaches saturation, collected MoS_2 nanoflakes gradually tend to obey Boltzmann distribution vertically subject to the force of gravity. And the simulation demonstrate the mechanism above successfully.

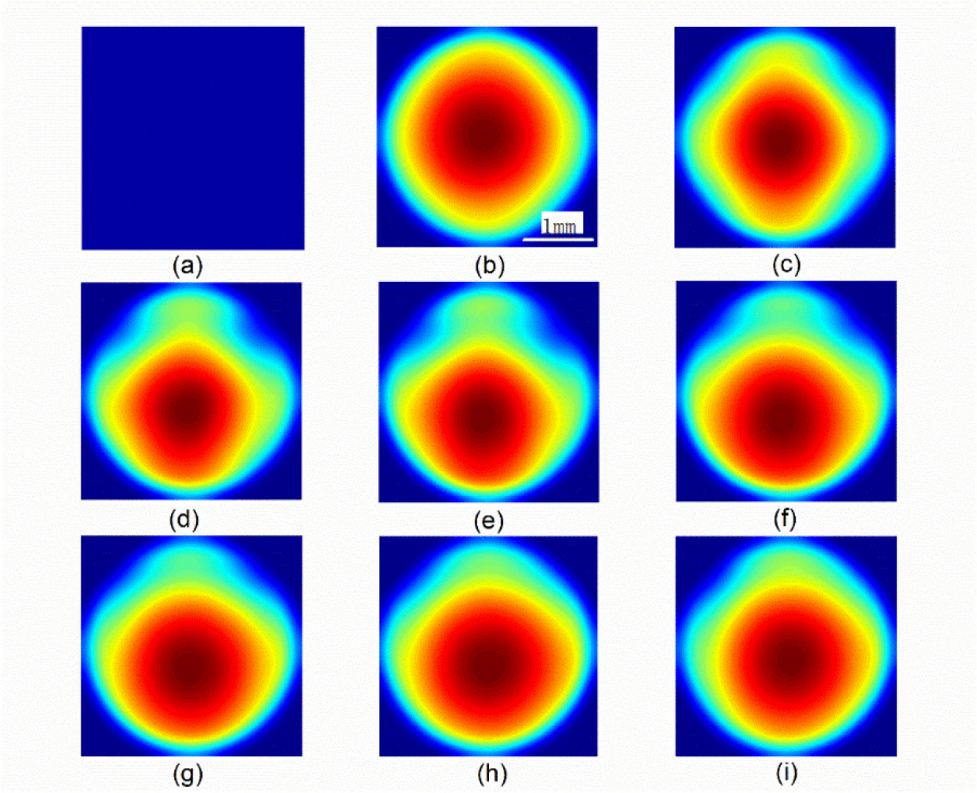

Fig. 5. (a) is the original distribution of MoS_2 in solution. Screenshots of dynamic self-diffraction video show in Figs. 4(b)-4(i) are used to retrieve the MoS_2 dynamic distribution show in Figs. 5(b)-5(i), respectively. (b) - (g), simulation of the second stage, indicate gathering center of MoS_2 nanoflakes start and gradually move at the direction of gravity. (g) - (i), simulation of the third stage, indicates that gathering center of MoS_2 moves horizontally.

3. Conclusion

We observe dynamic self-diffraction in MoS_2 supernatant solutions with laser for the first time, and conduct dynamic data simulation and analysis. Observation results indicate that self-diffraction can be divided in three stages: in the first stage, both the force of laser and viscous force of solution contribute to the mechanism. In the second stage, both the force of laser and gravity contribute to the mechanism. In the third stage, the mechanism is that fine structure of laser determines the shape of diffraction rings. Therefore, the fine structure of laser

#226987 - $15.00 USD Received 18 Nov 2014; revised 12 Feb 2015; accepted 18 Feb 2015; published 25 Feb 2015

can be observed by observation of diffraction pattern at the third stage by common CCD. Dynamic MoS_2 nanoflakes distribution in solution under the force of laser can be obtained by dynamic self-diffraction simulation. The relation between the forming of self-diffraction and laser power and MoS_2 nanoflake solution concentration can be demonstrated by static observation. The research sets the foundation for observation of nanomaterials' properties in solution by laser. And the application in liquid sample detection, nanomaterial detection, etc. would be promising.

Acknowledgments

Thanks for the extraordinary contributions of Dr. Daowei Wang to the theoretical analysis section of this paper.

This work was financially supported by the National Nature Science Foundation of China (11104356, 11404410, 11174371 and 11204112).

#226987 - $15.00 USD Received 18 Nov 2014; revised 12 Feb 2015; accepted 18 Feb 2015; published 25 Feb 2015